Published in final edited form as:
J Hepatol. 2013 November ; 59(5): 1007–1013. doi:10.1016/j.jhep.2013.06.010.

Regulation of accumulation and function of myeloid derived suppressor cells in different murine models of hepatocellular carcinoma

Tamar Kapanadze[1,2], **Jaba Gamrekelashvili**[1,2], **Chi Ma**[1], **Carmen Chan**[1], **Fei Zhao**[1], **Stephen Hewitt**[3], **Lars Zender**[4], **Veena Kapoor**[5], **Dean W. Felsher**[6], **Michael P. Manns**[2], **Firouzeh Korangy**[1,*], and **Tim F. Greten**[1,*]

[1] Gastrointestinal Malignancy Section, Medical Oncology Branch, National Cancer Institute, Bethesda, USA

[2] Department of Gastroenterology, Hepatology and Endocrinology, Hannover Medical School, Hannover, Germany

[3] Laboratory of Pathology, National Cancer Institute, NIH, Bethesda, USA

[4] Department of Gastroenterology, University of Tübingen, Tübingen, Germany

[5] Experimental Transplantation and Immunology Branch, NIH, Bethesda, USA

[6] Division of Medical Oncology, Department of Medicine, Stanford University, CA, USA

Abstract

Background and aims—Myeloid derived suppressor cells (MDSC) are immature myeloid cells with immunosuppressive activity. They accumulate in tumor-bearing mice and humans with different types of cancer, including hepatocellular carcinoma (HCC). The aim of this study was to examine the biology of MDSC in murine HCC models and to identify a model, which mimics the human disease.

Methods: The comparative analysis of MDSC was performed in mice, bearing transplantable, diethylnitrosoamine (DEN)-induced and MYC-expressing HCC at different ages.

Results: An accumulation of MDSC was found in mice with HCC irrespectively of the model tested. Transplantable tumors rapidly induced systemic recruitment of MDSC, in contrast to slow-growing DEN-induced or MYC-expressing HCC, where MDSC numbers only increased intra-hepatically in mice with advanced tumors. MDSC derived from mice with subcutaneous tumors were more suppressive than those from mice with DEN-induced HCC. Enhanced expression of genes associated with MDSC generation (GM-CSF, VEGF, IL-6, IL-1β) and migration (MCP-1, KC, S100A8, S100A9) was observed in mice with subcutaneous tumors. In contrast, only KC levels increased in mice with DEN-induced HCC. Both KC and GM-CSF over-expression or anti-KC and anti-GM-CSF treatment controlled MDSC frequency in mice with HCC. Finally, the frequency of MDSC decreased upon successful anti-tumor treatment with sorafenib.

Correspondence should be sent to: Tim F. Greten NIH/NCI/CCR Building 10 Rm. 12N226 9000 Rockville Pike Bethesda MD 20892 USA Telephone: 1 (301) 451 4723 Fax: 1 (301) 480 8780 tim.greten@nih.gov.

Conflict of Interest
The authors declare no competing financial interests

Conclusions: Our data indicate that MDSC accumulation is a late event during hepatocarcinogenesis and differs significantly depending on the tumor model studied.

Introduction

Myeloid derived suppressor cells (MDSC) represent a heterogeneous population of immature myeloid cells with suppressive activity. They include myeloid progenitors at various stages of differentiation, precursors of granulocytes, monocytes and dendritic cells (DC) [1]. In mice, MDSC are identified by co-expression of CD11b and Gr-1 and can be further divided into monocytic and granulocytic subtypes, depending on Ly6G/Ly6C or CD49d expression [2-4].

MDSC accumulate in spleen, blood and tumors of tumor-bearing animals [5]. Recently, they were also found in the liver of mice with subcutaneous tumors [6, 7]. MDSC suppress $CD8^+$ [8-10] and $CD4^+$ T cells [11] as well as NK [12, 13] cells through diverse mechanisms. Various tumor-derived soluble factors, including G-CSF, GM-CSF, VEGF, IL-6, IL-1β have been described to induce MDSC [1].

Analogues of murine MDSC have been found in blood and tumors of patients with various types of cancer [14]. We have previously described an increased frequency of $CD14^+HLA\text{-}DR^{low/neg.}$ cells in peripheral blood and tumors of patients with hepatocellular carcinoma (HCC), which not only suppressed T- and NK cells, but also induced $CD4^+CD25^+$ regulatory T cells [12, 15]. Various murine models of HCC have been developed, however, it remains questionable, which model mimics best the situation in patients and is useful for analysis of immune suppressor cells in HCC. With the aim to identify the best murine HCC tumor model which can be used to perform preclinical studies on MDSC, we performed comparative analysis in mice with carcinogen-induced, spontaneous and transplantable HCC.

We used a spontaneous HCC model, based on liver-specific inducible expression of human MYC [16]. Chemically induced HCC was established by injection of diethylnitrosamine (DEN) to two weeks old male mice [17]. Finally, we also injected two different HCC cell lines orthotopically or subcutaneously, in naïve mice, or as an “addon” to mice which already had DEN-induced HCC.

Materials and Methods

Cell lines

RIL-175 mouse hepatocellular carcinoma cell line was isolated from hepatic tumors established in C57BL/6 mice by transfer of $p53^{-/-}$ fetal hepatoblasts, transduced with $HRas^{v12}$ as previously described [18]. RIL-175-KC and RIL-175-GM-CSF cells were generated by transduction of RIL-175 with GM-CSF and KC expressing constructs. BNL cells were purchased from American Type Culture Collection. Sorafenib resistant BNL cells (BNL-R) were generated by growing BNL cells in the presence of 3μM sorafenib in vitro.

Animal Studies

C57BL/6 and Balb/c mice were obtained from Charles River (Sulzfeld, Germany) and NCI/Frederick (Frederick, USA). OVA-transgenic OT-I mice were from Jackson Laboratories (Bar Harbor, USA). LAP-tTA and TRE MYC mice were provided by Dr. Dean W. Felsher. MYC expression in the liver was activated by removing doxycycline treatment (100μg/ml) from the drinking water of 4 weeks old mice, transgenic for both TRE-MYC [16, 19] and LAP-tTA [20], as previously described [16]. Subcutaneous tumors were established by injection of 5×10^5-10^6 RIL-175, RIL-175-KC, RIL-175-GM-CSF, 1:1 mix of RIL-175-KC

and RIL-175-GM-CSF or 10^6 BNL cells in the right flank of mice. To induce orthotopic tumors, 5×10^5 RIL-175 cells (or phosphate buffered saline as a control) were injected under the liver capsule into the right liver lobe of anesthetized mice after subcostal laparatomy. Chemically induced HCC were established by intraperitoneal injection of diethylnitrosoamine (Sigma) in two-weeks-old male pups at a dose of 20μ g/g bodyweight. 10mg/kg Sorafenib (Bayer) was given daily by oral gavage.

Control mice received equal volume of the vehicle (Ethanol:Cremophor 1:1, 25% in dH_2O). 50μg anti-KC (R&D Systems), 100 μg anti-GM-CSF (R&D Systems) and rat IgG2a (R&D Systems) were injected 3x, intra-peritoneally every 3 days. Animals received human care according to institutional guidelines. All experimental protocols were approved by local Institutional Animal Care and Use Committees.

Cell isolation

Single cell suspensions were prepared from spleen, lymph nodes, liver and blood. The red blood cells were lysed by ACK Lysis Buffer (Quality Biologicals).

Flow Cytometry

Cells were stained with: anti-CD11b (Clone M1/70, Immunotools), anti-CD45 (clone 30-F11 eBioscience), anti-Gr-1 (clone RB6-8C5, Biolegend) and anti-CD8 (clone 53-6.7, eBioscience). Propidium iodide (Sigma) and 7AAD (BD Biosciense) were used for dead cell exclusion. Flow cytometry was performed on BD FacsCalibur (BD Biosciences). The data were analyzed using FlowJo software (Tree Star).

Purification of $CD11b^+Gr\text{-}1^+$ cells

Hepatic leukocytes were purified from the livers of tumor bearing mice as previously described [21] and labeled with anti-mouse CD11b-Microbeads (Miltenyi Biotec). $CD11b^+$ cells were isolated with AutoMacs, according to manufacturer's instructions and stained with anti-CD11b and anti-Gr-1. $CD11b^+Gr\text{-}1^+$ cells or $CD11b^+Gr\text{-}1^{high}$ and $CD11b^+Gr\text{-}1^{low}$ subsets were sorted on Influx™ Cell Sorter (BD Biosciences).

Suppression assay

$CD11b^+Gr\text{-}1^+$ cells or their subsets were isolated as indicated above and incubated with 1×10^5 CFSE (Molecular Probes)-labeled splenocytes from OT-I mice at indicated ratios in the presence of 0.1μ g/ml $OVA_{257\text{-}264}$ SIINFEKL peptide (Eurogentec). After 48hr of incubation, proliferation of $CFSE^+CD8^+$ cells was analyzed using flow cytometry.

Cytokine quantification

The serum samples were analyzed by Multiplex®MAP Mouse Cytokine/Chemokine kit (Millipore) according to manufacturer's instructions. Conditioned media, derived from *in vitro* cultured RIL-175 cells and explanted liver and tumor tissues were collected and analyzed for GM-CSF by ELISA (eBioscience) according to manufacturer's instructions. Amount of GM-CSF in the tissue culture supernatant was normalized to 1gram of tissue.

RNA isolation and Real-Time PCR

RNA was extracted from frozen tissues with RNeasyMini Kit (Qiagen). Complementary DNA was synthesized by iScript™cDNA synthesis kit (BioRad). Sequence of primers used for quantitative RT-PCR can be obtained from authors. The reactions were run in triplicates using iQSYBR green supermix kit (BioRad). The results were normalized to endogenous cyclophillin A expression levels. Naïve mouse liver was used as a calibrating sample. The data are shown in $2^{-\Delta\Delta Ct}$ format.

Statistical analysis

Experimental results are shown as Mean ± SEM. Significance of the difference between groups was calculated by Student's unpaired t-test and one-way ANOVA (Dunnett's and Bonferroni's multiple comparison test). $P<0.05$ was considered as statistically significant.

Results

Transplantable, carcinogen-induced and spontaneous HCC represent models of fast-growing and slow-growing tumors

We have compared tumor development in four different HCC models: mice with orthotopically or subcutaneously injected tumors, DEN induced tumors and spontaneous HCC in MYC ON mice. Injection of tumor cells subcutaneously or into the liver resulted in tumor development within 2-3 weeks. In contrast, MYC ON mice developed HCC 10 weeks after start of MYC expression and DEN-induced tumors were detected after 40 weeks of treatment (Table 1). While intra-hepatic injection of tumor cells led to infiltrative growth of tumor (Supplementary Fig. S1A), DEN-induced and MYC-expressing HCC were found to be more diffuse and distinct in livers forming nodules. Tumor occurrence was confirmed by microscopic analysis (Supplementary Fig. S1B, S1C).

Increased numbers of $CD11b^+Gr\text{-}1^+$ MDSC in mice with transplanted tumors

In order to study the role of $CD11b^+Gr\text{-}1^+$ cells in the development and growth of HCC, we performed comparative analysis of MDSC in all different liver tumor models. MDSC were identified as $CD11b^+Gr\text{-}1^+$ cells (Fig. 1A). As expected, increased relative and absolute numbers of $CD11b^+Gr\text{-}1^+$ cells were found in the spleen, blood and liver of C57BL/6 mice with orthotopic (Fig. 1B, 1C) and subcutaneous tumors (Fig. 1D, 1E). Similar results were obtained in Balb/c mice injected subcutaneously with BNL tumor cells (Fig. 1F). Unexpectedly, we did not find an increase in the number of hepatic and splenic $CD11b^+Gr\text{-}1^+$ cells in mice with tumors at 40 weeks after DEN treatment in comparison to naïve age-matched control (Fig. 1D, 1E). Similarly, MYC ON mice did not show accumulation of MDSC 10 weeks after initiation of MYC expression, when mice started to develop HCC (Fig. 1G).

MDSC increase in livers of mice with advanced DEN-induced and MYC expressing HCC

Since we did not observe a change in numbers of MDSC in DEN-treated and MYC ON mice at early stages of HCC, we decided to wait longer until mice have advanced disease and large tumors. This was also supported by the fact that most studies including our own on MDSC in patients with HCC [12, 15] restrict their analysis to patients with advanced disease. We observed a further progression of primary tumors in DEN treated mice and 33% of all mice developed macroscopically lung metastasis at 72 weeks after DEN treatment (Supplementary Fig. S2A, S2B). Progressive growth of the tumors was confirmed by an increase of the body weight/liver weight ratio (BLR) in DEN-treated animals after 56, 64 and 72 weeks of DEN-injection (Supplementary Fig. S2C). Analysis of MDSC in mice with further advanced disease indicated an increase in the number of tumor infiltrating MDSC, which paralleled BLR dynamics (Fig. 2A). However, no significant increase in splenic MDSC was observed (Fig. 2B). Subpopulation analysis revealed that both $CD11b^+Gr\text{-}1^{high}$ granulocytic and $CD11b^+Gr\text{-}1^{low}$ monocytic MDSC were increased in the liver 72 weeks after DEN treatment, whereas only $CD11b^+Gr\text{-}1^{high}$ showed significant increase in the spleen (Fig. 2C, 2D). Similarly, MYC ON mice showed high numbers of MDSC 13 weeks after starting of MYC expression (Fig. 2E), when tumors had already reached an advanced stage, as confirmed by increased BLR (Supplementary Fig. S2D, S2E).

Subcutaneously growing tumors trigger accumulation of MDSC in mice with DEN-induced HCC

So far our data indicated that besides liver, MDSC accumulated in the spleen of mice bearing subcutaneous or orthotopic tumors, but not in mice with chemically induced HCC. In order to distinguish whether DEN-induced tumors trigger or inhibit accumulation of MDSC, we next injected RIL-175 cells subcutaneously into mice with DEN-induced HCC. Frequencies of MDSC were determined when subcutaneous tumors reached 10 to 15 mm in size. Injection of RIL-175 caused similar increase in the relative and absolute MDSC numbers in spleen, blood and liver of mice with DEN-induced tumors (Fig. 3A, 3B). Furthermore, the frequency of MDSC was similar in RIL-175 injected mice with and without DEN-induced HCC (data not shown).

Transplanted tumors induce more suppressive MDSC than chemically-induced HCC

Next, we tested the function of hepatic MDSC derived from mice with subcutaneous tumors and tumor infiltrating MDSC from mice with DEN-induced HCC and mice with DEN induced HCC, which also grew subcutaneous tumor transplants. Purified hepatic $CD11b^{+}Gr\text{-}1^{+}$ cells were incubated for 48hr with $OVA_{257\text{-}264}$ peptide-stimulated OT-I splenocytes in order to test the suppressor activity. MDSC from mice with DEN induced HCC were less suppressive than MDSC from mice with subcutaneous tumors. Interestingly, the most efficient suppressors were $CD11b^{+}Gr\text{-}1^{+}$ cells, obtained from mice with DEN induced tumor, which were also challenged with subcutaneous tumors (Fig. 3C). Subset analysis indicated a higher ratio of monocytic:granulocytic MDSC in mice with subcutaneously growing tumors than in mice with DEN induced HCC without additional subcutaneous tumors (Fig. 3D). Monocytic MDSC have been shown to be more suppressive in other tumor models [4]. Similar results can be found in mice with subcutaneous HCC. Suppressive activity of both-granulocytic and monocytic MDSC was dependent on expression of iNOS, but independent from arginase (Supplementary Fig. S3A).

Subcutaneously growing tumors express more GM-CSF, G-CSF, VEGF and MCP-1

In order to better understand the biology of MDSC accumulation in the different HCC models, we performed gene expression analysis. MRNA was isolated from DEN induced- and subcutaneous RIL-175 tumors and screened for expression of factors known to be relevant for the generation (G-CSF, GM-CSF, M-CSF, IL-6, IL-1β,) [22-27] and migration (KC, MCP-1, S100A8, S100A9) [7, 23, 28] of MDSC. Enhanced expression of IL-6, S100A8, S100A9, KC, MCP-1 was found in liver tumors from mice at 72 weeks after DEN-treatment (Fig. 4A). In contrast, subcutaneously growing tumors were also expressing G-CSF, GM-CSF, IL-1β and VEGF (Fig. 4B). Interestingly, we found increased expression of KC, IL-6, MCP-1, S100A8 and S100A9 even in the liver of mice with subcutaneous tumors (Fig. 4C), which could explain the increase of hepatic MDSC in this model. Tumor-derived GM-CSF has been reported to trigger accumulation of MDSC in the spleen of tumor bearing mice [9, 24]. Screening of tumor-conditioned media, derived from RIL-175 cells revealed time-dependent increase of GM-CSF (Supplementary Fig. S4A). Furthermore, high amount of GM-CSF was also found in explanted RIL-175 tumor tissues *in vitro* (Supplementary Fig. S4B). Screening of sera revealed that DEN-treated mice showed time dependent increase of KC levels (Supplementary Fig. S4C, which correlated with increased numbers of $CD11b^{+}Gr\text{-}1^{+}$ cells in the liver (Fig. 2A). Less intensive but significant increase of KC amounts was also found in the sera of mice with subcutaneous tumors (Supplementary Fig. S4D).

To study the role of KC and GM-CSF in generation and/or recruitment of MDSC *in vivo*, we injected subcutaneous tumor bearing mice with anti-KC or anti-GM-CSF neutralizing antibodies. Reduced numbers of $CD11b^{+}Gr1^{+}$ cells were found upon anti-KC and anti-GM-

CSF treatment (Fig. 4D). Next, we established subcutaneous tumors by injection of wild type (WT), KC- and GM-CSF over-expressing RIL-175 cells. Mice with KC and GM-CSF over-expressing tumors developed higher numbers of MDSC in the spleen and liver, as compared to animals injected with wild type RIL-175. Interestingly, mixing KC and GM-CSF over-expressing tumors only marginally increased the frequency of hepatic and splenic MDSC (Fig. 4E). Similar results were found when tumor infiltrating MDSC were analyzed (Supplementary Fig. S5). Finally, we investigated the effect of systemic sorafenib administration on MDSC frequencies. Sorafenib treatment delayed tumor growth (Fig. 4F) in BNL tumor-bearing mice, accompanied by a reduction in MDSC frequency (Fig. 4G). This effect was not seen when the treatment was administered into mice injected with a sorafenib-resistant tumor cell line (BNL-R), suggesting, that HCC directly controls expansion of MDSC rather than a direct effect of sorafenib on MDSC as previously suggested [29].

Discussion

MDSC have been an area of intense research in the last years, due to their strong immune suppressor function in patients with cancer [1, 14]. Murine tumor models are widely used to study the interaction between cancer and immune function. Transplantable tumor models are frequently used to study MDSC biology [1, 30, 31], however, they have a number of disadvantages. Results are highly dependent on the tumor cell line used. The dynamics and latency of tumor growth is not comparable to the situation in humans and finally, subcutaneous transplants grow independently from the organ of interest [32].

We have previously shown an increase in the frequency of $CD14^{+}HLA\text{-}DR^{low/neg.}$ MDSC in patients with HCC and showed that these cells induced Foxp3 expression in $CD4^{+}$ T cells [15] and suppressed NK cell function *in vitro* [12]. In order to better understand the complex immunobiology of MDSC in HCC, we decided to test MDSC in four different HCC models: chemically induced HCC [17], spontaneous HCC in mice expressing human MYC [16] and two transplantation models in which syngeneic tumor cell lines were injected subcutaneously or into the liver. DEN- and MYC-induced HCC have been suggested to be comparable with human HCC [33].

We examined frequency, subtype distribution and function of MDSC as well as factors responsible for their recruitment at early and late stages of HCC. As expected, all tumor bearing mice demonstrated elevated MDSC frequencies. However, closer analysis demonstrated subtle differences in frequency and location of MDSC. An increase in splenic and hepatic MDSC was found in mice with subcutaneous tumors. In contrast, mice with early stages of chemically induced or MYC dependent HCC showed normal MDSC numbers confirming results obtained in $D6^{-/-}$ mice with knockout of chemokine scavenging receptor [34].

The majority of published studies on human MDSC have been done using blood samples from patients with advanced disease [14]. Frequency of MDSC was found to correlate with tumor stage [35] and MDSC have been suggested as an independent prognostic factor for poor survival in patients with gastrointestinal cancer [36]. This prompted us to study MDSC in mice with late stage DEN- and MYC-induced HCC where we found an increase of liver infiltrating MDSC in mice with advanced disease.

Until today the reasons for accumulation of MDSC are not completely understood. One could speculate that cytokines and/or chemokines released by subcutaneous tumors differ from those of spontaneous tumors. Several factors produced by tumors have been described to induce an accumulation or migration of tumor derived MDSC. GM-CSF [24, 37, 38] G-

CSF [22, 27], IL-1β [26], IL-6 [25], VEGF [39], have been described to cause an accumulation of MDSC, while S100A8/A9 [23], KC [7] and MCP-1 [28], have been shown to regulate their migration. Both increased serum GM-CSF and KC levels have been described in patients with HCC [40]. We have tested the expression of these cytokines in subcutaneous and DEN induced tumors. GM-CSF was the only cytokine, which was expressed by tumor cells and which could be detected in subcutaneous tumors. Therefore, our data suggests that GM-CSF expression by tumors is responsible for systemic accumulation of MDSC in the models described.

Gene expression studies indicated an over-expression of MCP-1, S100A8/9 and KC in DEN induced tumors. Interestingly, we found a direct correlation between the increase of KC and hepatic MDSC frequency, which was not observed with all other cytokines tested. KC (CXCL1) belongs to the CXC chemokine family and can be found at increased levels in tumor bearing mice. This can lead to an accumulation of hepatic MDSC [7]. We noticed increased KC expression not only in livers of animals with primary HCC, but also in tumor free livers from mice with subcutaneous tumors, suggesting that KC might control migration of MDSC specifically into the liver. It should be noted that due to the infiltrative and disseminated tumor growth in DEN treated mice, it was not possible to separate primary liver tumors from non-tumor liver tissue.

Finally, our study demonstrated a functional difference of hepatic MDSC, which include tumor infiltrating cells, in mice with DEN-induced HCC and transplanted tumors. Based on previous studies indicating that tumor infiltrating MDSC differ from MDSC derived from peripheral lymphoid organs [41], we focused our studies on tumor infiltrating, hepatic MDSC. *In vitro* suppression analysis of $CD11b^{+}Gr\text{-}1^{+}$ MDSC from mice with DEN-induced tumors showed them to be less suppressive than MDSC from mice with subcutaneously growing tumors. This was potentially caused by a difference in the proportion of monocytic and granulocytic MDSC in mice with subcutaneous tumors, which have been described to differ in their suppressor activity [4].

In summary, we have shown that the frequency and function of MDSC in HCC bearing mice depend on the tumor model chosen, stage of the disease and is controlled by soluble factors, derived from tumors or produced by the tumor microenvironment. Our data supports previous studies using subcutaneous tumor models suggesting that MDSC frequency correlate with cytokines produced by tumors and therefore also correlate with tumor mass [9]. Different tumor models should be chosen to study MDSC biology in mice since no single model mimics the situation in patients completely. This information is of particular importance for future studies, which aim to translate information gained from murine preclinical studies to clinical settings of HCC and potentially other types of cancer.

Supplementary Material

Refer to Web version on PubMed Central for supplementary material.

Acknowledgments

We would like to thank Dr. Leigh Samsel (National Institute of Heart, Blood and Lung) for help with luminex assays.

Financial Support

The research was supported (in part) by the Intramural Research Program of the NIH, National Cancer Institute, Center for Cancer Research and by the Networking Fund of the Helmholtz Association within the Helmholtz Alliance on Immunotherapy of Cancer to MPM.

Abbreviations

BLR	body weight/liver weight ratio
DEN	diethylnitrosoamine
G-CSF	granulocyte colony stimulating factor
GM-CSF	granulocyte-macrophage colony stimulating factor
HCC	hepatocellular carcinoma
IL	interleukin
iNOS	inducible nitric oxide synthase
KC	keratinocyte-derived chemokine
LAP	liver activator protein
L-NMMA-N^{G}	methyl-L-arginine
MCP	macrophage chemotactic protein
MDSC	myeloid derived suppressor cell
NK	natural killer
N-NOHA-N $^{\omega}$	hydroxil-nor-L-arginine
OVA	ovalbumin
VEGF	vascular endothelial growth factor
WT	wild type)

References

1. Gabrilovich DI, Nagaraj S. Myeloid-derived suppressor cells as regulators of the immune system. Nat Rev Immunol. 2009; 9:162–174. [PubMed: 19197294]
2. Movahedi K, Guilliams M, Van den Bossche J, Van den Bergh R, Gysemans C, Beschin A, et al. Identification of discrete tumor-induced myeloid-derived suppressor cell subpopulations with distinct T cell-suppressive activity. Blood. 2008; 111:4233–4244. [PubMed: 18272812]
3. Youn JI, Nagaraj S, Collazo M, Gabrilovich DI. Subsets of myeloid-derived suppressor cells in tumor-bearing mice. J Immunol. 2008; 181:5791–5802. [PubMed: 18832739]
4. Haile LA, Gamrekelashvili J, Manns MP, Korangy F, Greten TF. CD49d is a new marker for distinct myeloid-derived suppressor cell subpopulations in mice. J Immunol. 2010; 185:203–210. [PubMed: 20525890]
5. Gabrilovich DI, Bronte V, Chen SH, Colombo MP, Ochoa A, Ostrand-Rosenberg S, et al. The terminology issue for myeloid-derived suppressor cells. Cancer Res. 2007; 67:425. author reply 426. [PubMed: 17210725]
6. Ilkovitch D, Lopez DM. The liver is a site for tumor-induced myeloid-derived suppressor cell accumulation and immunosuppression. Cancer Res. 2009; 69:5514–5521. [PubMed: 19549903]
7. Connolly MK, Mallen-St Clair J, Bedrosian AS, Malhotra A, Vera V, Ibrahim J, et al. Distinct populations of metastases-enabling myeloid cells expand in the liver of mice harboring invasive and preinvasive intra-abdominal tumor. J Leukoc Biol. 2010; 87:713–725. [PubMed: 20042467]
8. Gabrilovich DI, Velders MP, Sotomayor EM, Kast WM. Mechanism of immune dysfunction in cancer mediated by immature Gr-1+ myeloid cells. J Immunol. 2001; 166:5398–5406. [PubMed: 11313376]
9. Bronte V, Chappell DB, Apolloni E, Cabrelle A, Wang M, Hwu P, et al. Unopposed production of granulocyte-macrophage colony-stimulating factor by tumors inhibits CD8+ T cell responses by dysregulating antigen-presenting cell maturation. J Immunol. 1999; 162:5728–5737. [PubMed: 10229805]

10. Kusmartsev S, Nefedova Y, Yoder D, Gabrilovich DI. Antigen-specific inhibition of CD8+ T cell response by immature myeloid cells in cancer is mediated by reactive oxygen species. J Immunol. 2004; 172:989–999. [PubMed: 14707072]
11. Nagaraj S, Gabrilovich DI. Regulation of suppressive function of myeloid-derived suppressor cells by CD4(+) T cells. Semin Cancer Biol. 2012
12. Hoechst B, Voigtlaender T, Ormandy L, Gamrekelashvili J, Zhao F, Wedemeyer H, et al. Myeloid derived suppressor cells inhibit natural killer cells in patients with hepatocellular carcinoma via the NKp30 receptor. Hepatology. 2009; 50:799–807. [PubMed: 19551844]
13. Li H, Han Y, Guo Q, Zhang M, Cao X. Cancer-expanded myeloid-derived suppressor cells induce anergy of NK cells through membrane-bound TGF-beta 1. J Immunol. 2009; 182:240–249. [PubMed: 19109155]
14. Greten TF, Manns MP, Korangy F. Myeloid derived suppressor cells in human diseases. Int Immunopharmacol. 2011; 11:802–807. [PubMed: 21237299]
15. Hoechst B, Ormandy LA, Ballmaier M, Lehner F, Kruger C, Manns MP, et al. A new population of myeloid-derived suppressor cells in hepatocellular carcinoma patients induces CD4(+)CD25(+)Foxp3(+) T cells. Gastroenterology. 2008; 135:234–243. [PubMed: 18485901]
16. Shachaf CM, Kopelman AM, Arvanitis C, Karlsson A, Beer S, Mandl S, et al. MYC inactivation uncovers pluripotent differentiation and tumour dormancy in hepatocellular cancer. Nature. 2004; 431:1112–1117. [PubMed: 15475948]
17. Vesselinovitch SD, Mihailovich N. Kinetics of diethylnitrosamine hepatocarcinogenesis in the infant mouse. Cancer Res. 1983; 43:4253–4259. [PubMed: 6871863]
18. Zender L, Xue W, Cordon-Cardo C, Hannon GJ, Lucito R, Powers S, et al. Generation and analysis of genetically defined liver carcinomas derived from bipotential liver progenitors. Cold Spring Harb Symp Quant Biol. 2005; 70:251–261. [PubMed: 16869761]
19. Cao Z, Fan-Minogue H, Bellovin DI, Yevtodiyenko A, Arzeno J, Yang Q, et al. MYC phosphorylation, activation, and tumorigenic potential in hepatocellular carcinoma are regulated by HMG-CoA reductase. Cancer Res. 2011; 71:2286–2297. [PubMed: 21262914]
20. Kistner A, Gossen M, Zimmermann F, Jerecic J, Ullmer C, Lubbert H, et al. Doxycycline-mediated quantitative and tissue-specific control of gene expression in transgenic mice. Proc Natl Acad Sci U S A. 1996; 93:10933–10938. [PubMed: 8855286]
21. Ma C, Kapanadze T, Gamrekelashvili J, Manns MP, Korangy F, Greten TF. Anti-Gr-1 antibody depletion fails to eliminate hepatic myeloid-derived suppressor cells in tumor-bearing mice. J Leukoc Biol. 2012; 92:1199–1206. [PubMed: 23077247]
22. Waight JD, Hu Q, Miller A, Liu S, Abrams SI. Tumor-derived G-CSF facilitates neoplastic growth through a granulocytic myeloid-derived suppressor cell-dependent mechanism. PLoS One. 2011; 6:e27690. [PubMed: 22110722]
23. Sinha P, Okoro C, Foell D, Freeze HH, Ostrand-Rosenberg S, Srikrishna G. Proinflammatory S100 proteins regulate the accumulation of myeloid-derived suppressor cells. J Immunol. 2008; 181:4666–4675. [PubMed: 18802069]
24. Serafini P, Carbley R, Noonan KA, Tan G, Bronte V, Borrello I. High-dose granulocyte-macrophage colony-stimulating factor-producing vaccines impair the immune response through the recruitment of myeloid suppressor cells. Cancer Res. 2004; 64:6337–6343. [PubMed: 15342423]
25. Cheng L, Wang J, Li X, Xing Q, Du P, Su L, et al. Interleukin-6 induces Gr-1+CD11b+ myeloid cells to suppress CD8+ T cell-mediated liver injury in mice. PLoS One. 2011; 6:e17631. [PubMed: 21394214]
26. Bunt SK, Sinha P, Clements VK, Leips J, Ostrand-Rosenberg S. Inflammation induces myeloid-derived suppressor cells that facilitate tumor progression. J Immunol. 2006; 176:284–290. [PubMed: 16365420]
27. Abe F, Dafferner AJ, Donkor M, Westphal SN, Scholar EM, Solheim JC, et al. Myeloid-derived suppressor cells in mammary tumor progression in FVB Neu transgenic mice. Cancer Immunol Immunother. 2010; 59:47–62. [PubMed: 19449184]

28. Sawanobori Y, Ueha S, Kurachi M, Shimaoka T, Talmadge JE, Abe J, et al. Chemokine-mediated rapid turnover of myeloid-derived suppressor cells in tumor-bearing mice. Blood. 2008; 111:5457–5466. [PubMed: 18375791]
29. Cao M, Xu Y, Youn JI, Cabrera R, Zhang X, Gabrilovich D, et al. Kinase inhibitor Sorafenib modulates immunosuppressive cell populations in a murine liver cancer model. Lab Invest. 2011; 91:598–608. [PubMed: 21321535]
30. Ostrand-Rosenberg S, Sinha P, Beury DW, Clements VK. Cross-talk between myeloid-derived suppressor cells (MDSC), macrophages, and dendritic cells enhances tumor-induced immune suppression. Semin Cancer Biol. 2012
31. Ribechini E, Greifenberg V, Sandwick S, Lutz MB. Subsets, expansion and activation of myeloid-derived suppressor cells. Med Microbiol Immunol. 2010; 199:273–281. [PubMed: 20376485]
32. Heindryckx F, Colle I, Van Vlierberghe H. Experimental mouse models for hepatocellular carcinoma research. Int J Exp Pathol. 2009; 90:367–386. [PubMed: 19659896]
33. Farazi PA, DePinho RA. Hepatocellular carcinoma pathogenesis: from genes to environment. Nat Rev Cancer. 2006; 6:674–687. [PubMed: 16929323]
34. Schneider C, Teufel A, Yevsa T, Staib F, Hohmeyer A, Walenda G, et al. Adaptive immunity suppresses formation and progression of diethylnitrosamine-induced liver cancer. Gut. 2012
35. Diaz-Montero CM, Salem ML, Nishimura MI, Garrett-Mayer E, Cole DJ, Montero AJ. Increased circulating myeloid-derived suppressor cells correlate with clinical cancer stage, metastatic tumor burden, and doxorubicin-cyclophosphamide chemotherapy. Cancer Immunol Immunother. 2009; 58:49–59. [PubMed: 18446337]
36. Gabitass RF, Annels NE, Stocken DD, Pandha HA, Middleton GW. Elevated myeloid-derived suppressor cells in pancreatic, esophageal and gastric cancer are an independent prognostic factor and are associated with significant elevation of the Th2 cytokine interleukin-13. Cancer Immunol Immunother. 2011; 60:1419–1430. [PubMed: 21644036]
37. Bayne LJ, Beatty GL, Jhala N, Clark CE, Rhim AD, Stanger BZ, et al. Tumor-derived granulocyte-macrophage colony-stimulating factor regulates myeloid inflammation and T cell immunity in pancreatic cancer. Cancer Cell. 2012; 21:822–835. [PubMed: 22698406]
38. Dolcetti L, Peranzoni E, Ugel S, Marigo I, Fernandez Gomez A, Mesa C, et al. Hierarchy of immunosuppressive strength among myeloid-derived suppressor cell subsets is determined by GM-CSF. Eur J Immunol. 2010; 40:22–35. [PubMed: 19941314]
39. Gabrilovich D, Ishida T, Oyama T, Ran S, Kravtsov V, Nadaf S, et al. Vascular endothelial growth factor inhibits the development of dendritic cells and dramatically affects the differentiation of multiple hematopoietic lineages in vivo. Blood. 1998; 92:4150–4166. [PubMed: 9834220]
40. Capone F, Costantini S, Guerriero E, Calemma R, Napolitano M, Scala S, et al. Serum cytokine levels in patients with hepatocellular carcinoma. Eur Cytokine Netw. 2010; 21:99–104. [PubMed: 20478763]
41. Corzo CA, Condamine T, Lu L, Cotter MJ, Youn JI, Cheng P, et al. HIF-1alpha regulates function and differentiation of myeloid-derived suppressor cells in the tumor microenvironment. J Exp Med. 2010; 207:2439–2453. [PubMed: 20876310]

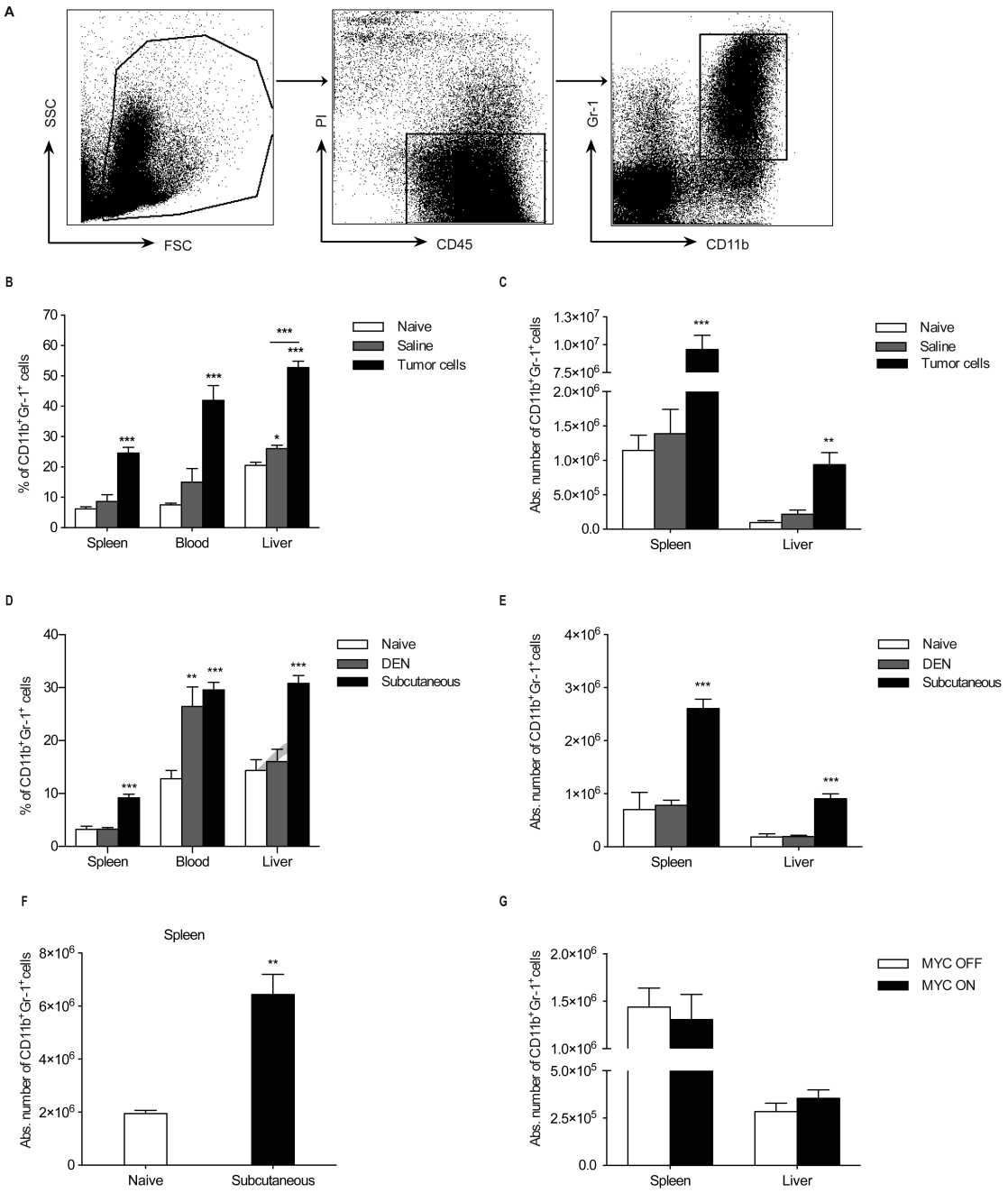

Fig. 1. MDSC analysis in murine HCC models

(A) Representative flow cytometric analysis of liver $CD11b^+Gr\text{-}1^+$ cells. (B-F) Analysis of $CD11b^+Gr\text{-}1^+$ cells in female mice with transplantable orthotopic (B, C) and in male mice with subcutaneous (D, E, F), DEN-induced (D, E) and MYC-expressing (G) liver tumors. Relative numbers of $CD11b^+Gr\text{-}1^+$ cells are shown as a percentage of live $CD45^+$ cells. Absolute numbers were determined per spleen or per gram of liver tissue. (B-C) N=4 naïve, N=4 saline- and N=6 RIL-175-injected mice; (D-E) N=9 naïve, N=12 DEN-induced- and N=8 subcutaneous tumor bearing mice; (F) N=5 naïve and N=13 BNL tumor bearing mice, (G) N=4 MYC OFF and N=5 MYC ON mice . All data are expressed as mean ± SEM and

are cumulative of three independent experiments. *P<0.05, **P<0.01, ***P<0.001: Student's t test.

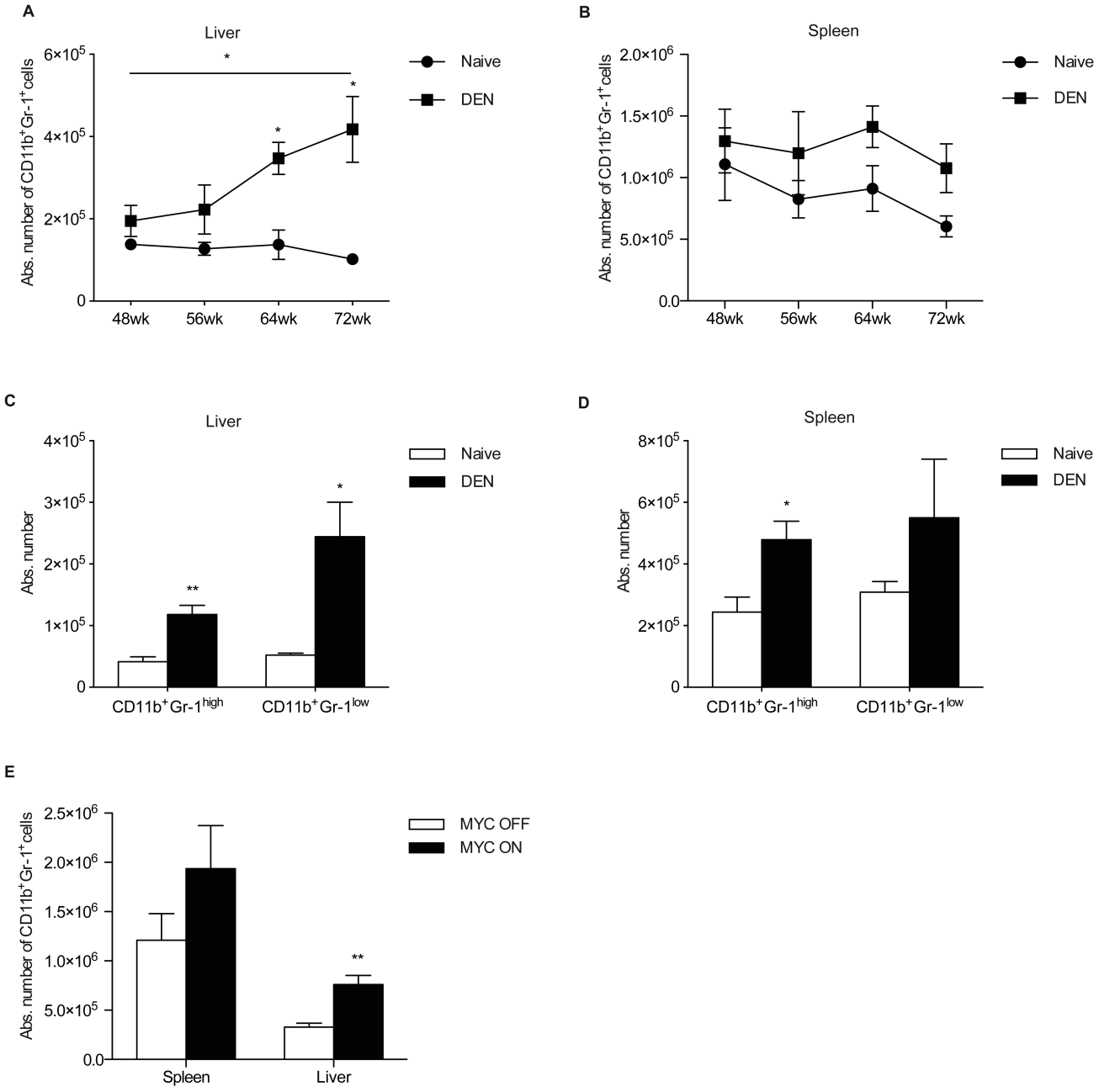

Fig. 2. MDSC accumulate in mice with HCC over time

(A-B) $CD11b^+Gr\text{-}1^+$ cells in the liver (A) and spleen (B) of tumor bearing mice 48 (N=11), 56 (N=6), 64 (N=9) and 72 (N=6) weeks after DEN injection. (C-D) Absolute numbers of $CD11b^+Gr\text{-}1^{high}$ and $CD11b^+Gr\text{-}1^{low}$cells in the liver (C) and spleen (D) of mice 72 weeks after DEN injection. (E) $CD11b^+Gr\text{-}1^+$ cells in MYC ON mice at 13 weeks after initiation of MYC expression. The data are expressed as mean ± SEM and are cumulative of at least 3 independent experiments. **P*<0.05, ***P*<0.01, ****P*<0.001: Student's t test.

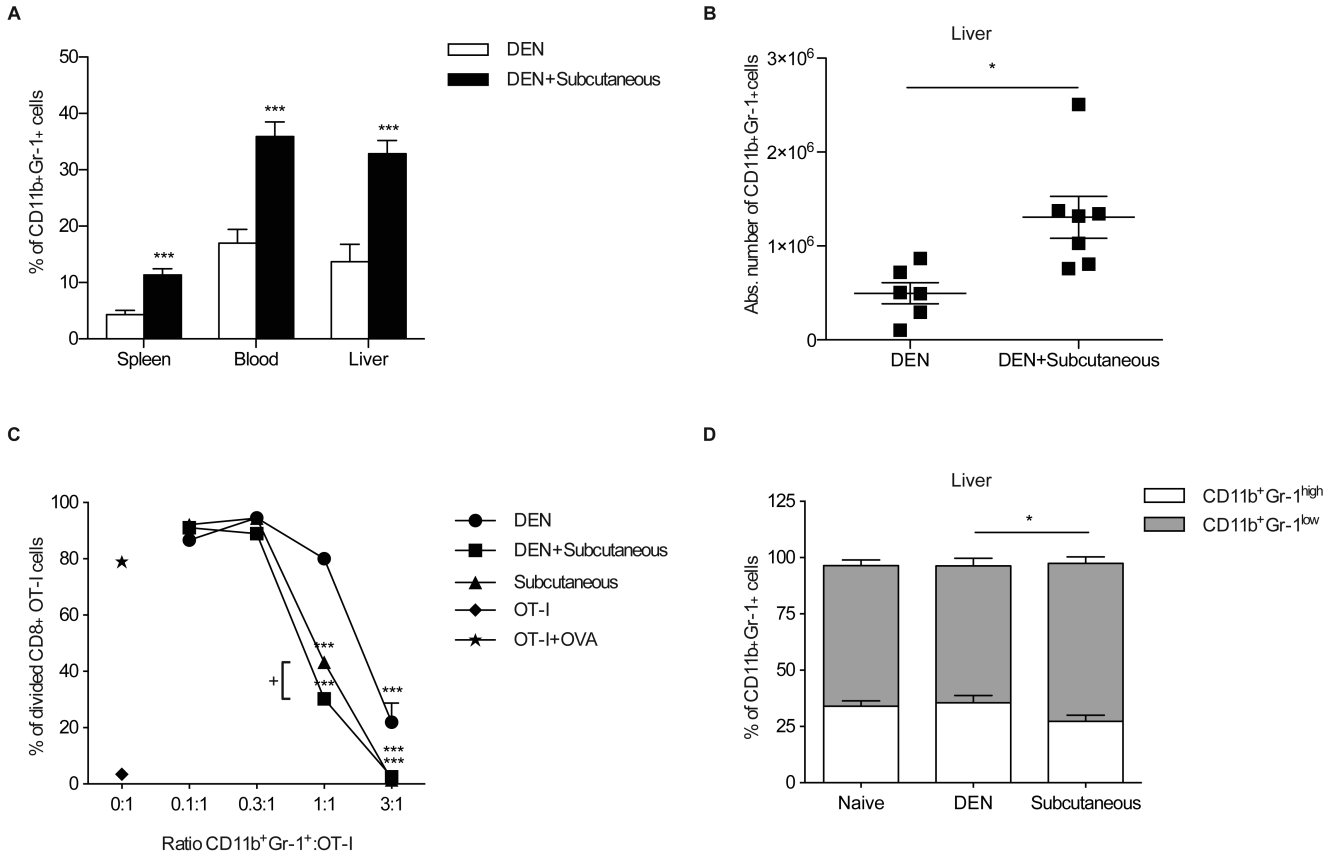

Fig. 3. Subcutaneously growing tumors control frequency and function of MDSC in mice with DEN-induced HCC

Relative (A) and absolute (B) numbers of MDSC in DEN-treated mice with or without subcutaneous RIL-175 tumors. (C) Proliferation of OT-I T cells after co-culture with hepatic $CD11b^{+}Gr\text{-}1^{+}$ cells from subcutaneous RIL-175 tumor bearing and DEN-treated mice with and without subcutaneous RIL-175 tumors. (D) Relative distribution of $CD11b^{+}Gr\text{-}1^{high}$ and $CD11b^{+}Gr\text{-}1^{low}$ subpopulations in total hepatic $CD11b^{+}Gr\text{-}1^{+}$ cells (N=11 naïve, N=9 DEN-induced- and N=11 subcutaneous tumor bearing mice). Data are expressed as mean ± SEM. *P<0.05, ***P<0.001: Student's t test (A, B, D) and 1-way ANOVA with Dunnett's and Bonferroni's multiple comparison tests (C). +P<0.001

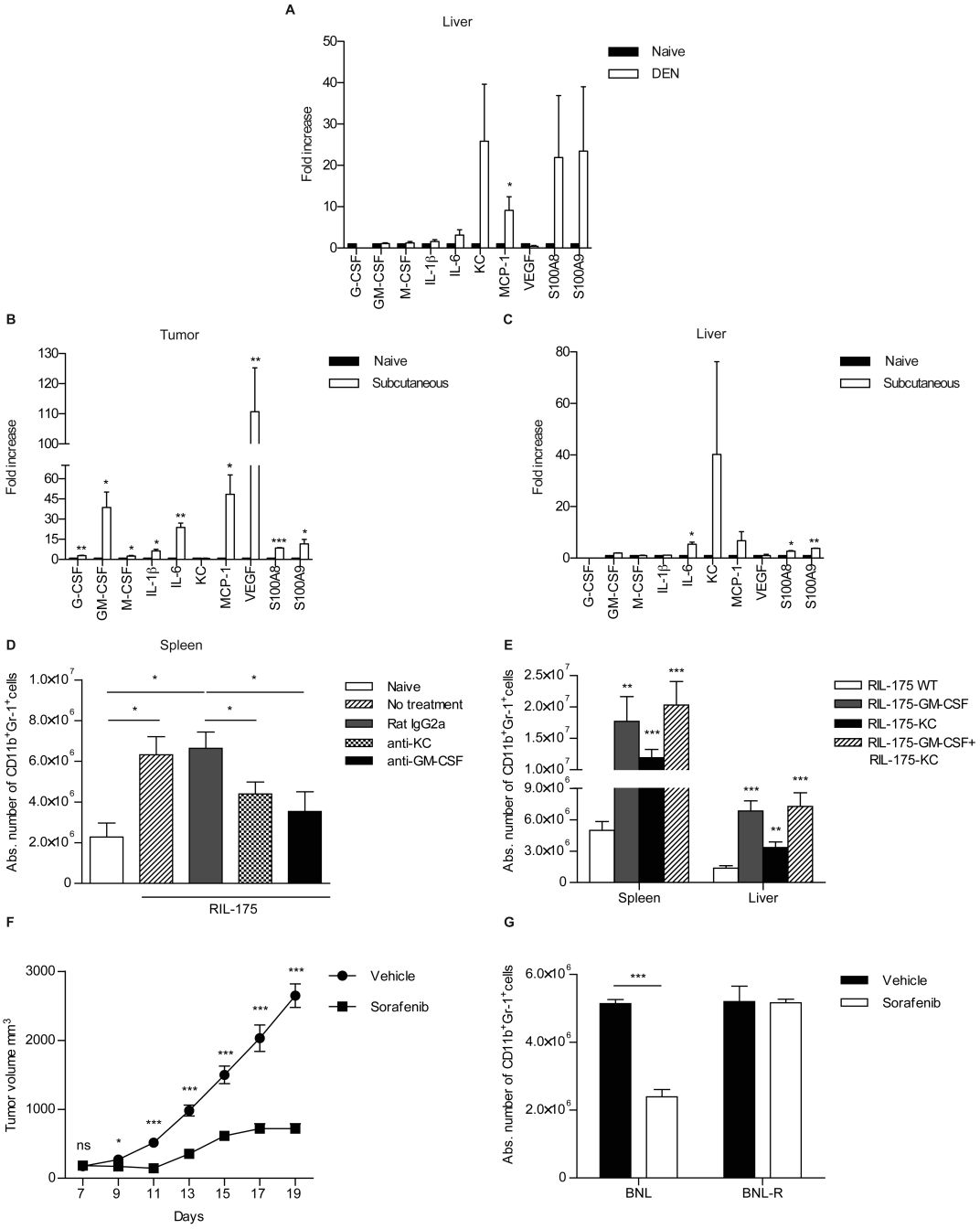

Fig. 4. Recruitment of MDSC is controlled by GM-CSF and KC

(A-C) Cytokine expression analysis in mice with DEN-induced (A) and subcutaneous RIL-175 (B,C) tumors. (D-E) Numbers of $CD11b^{+}Gr\text{-}1^{+}$ cells: (D) in mice with subcutaneous HCC after anti-KC and anti-GM-CSF treatment; (E) after establishment of GM-CSF- and KCoverexpressing HCC and their mix. (F-G) Effect of systemic sorafenib treatment: (F) tumor growth kinetics (vehicle: N=14, sorafenib: N=10)) (G) frequency of $CD11b^{+}Gr\text{-}1^{+}$ cells in mice with sorafenib-sensitive and sorafenib-resistant tumors. Data are expressed as mean ± SEM and are cumulative of 2 independent experiments, $*P<0.05$, $**P<0.01$, $***P<0.001$: Student's t test.

Table 1

HCC incidence in different tumor models

Time	Tumor model					
	Transplantable		MYC ON		DEN-induced	
	Subcutaneous	Orthotopic	N	% of total	N	% of total
1 week	8/8	n/a	n/a	n/a	0/32	0 %
2 weeks	8/8	6/6	n/a	n/a	0/32	0 %
16 weeks	n/a	n/a	10/10	100%	0/6	0%
40 weeks	n/a	n/a	n/a	n/a	10/12	83%
48 weeks	n/a	n/a	n/a	n/a	12/12	100 %